New proton radioactivities ^{165,166,167}Ir and ^{171}Au

C. N. Davids,[1] P. J. Woods,[2] J. C. Batchelder,[3] C. R. Bingham,[4,5] D. J. Blumenthal,[1] L. T. Brown,[1,6] B. C. Busse,[7] L. F. Conticchio,[8] T. Davinson,[2] S. J. Freeman,[9] D. J. Henderson,[1] R. J. Irvine,[2] R. D. Page,[2] H. T. Penttilä,[1,8] D. Seweryniak,[1,8] K. S. Toth,[5] W. B. Walters,[8] and B. E. Zimmerman[4]

[1]*Argonne National Laboratory, Argonne, Illinois 60439*
[2]*University of Edinburgh, Edinburgh, United Kingdom*
[3]*Louisiana State University, Baton Rouge, Louisiana 70803*
[4]*University of Tennessee, Knoxville, Tennessee 37996*
[5]*Oak Ridge National Laboratory, Oak Ridge, Tennessee 37831*
[6]*Vanderbilt University, Nashville, Tennessee 37235*
[7]*Oregon State University, Corvallis, Oregon 97331*
[8]*University of Maryland, College Park, Maryland 20742*
[9]*University of Manchester, Manchester, United Kingdom*

(Received 13 January 1997)

The new proton radioactivities ^{165,166,167}Ir and ^{171}Au have been observed. The Ir isotopes were produced *via* the ^{92}Mo(^{78}Kr,pxn)^{165,166,167}Ir reactions at 357 and 384 MeV. ^{171}Au was produced *via* the ^{96}Ru(^{78}Kr,$p2n$)^{171}Au reaction at 389 MeV. The proton emitters were each identified by position, time, and energy correlations between the implantation of a residual nucleus into a double-sided silicon strip detector, the observation of a decay proton, and the subsequent observation of a decay alpha particle from the daughter nucleus (^{164,165,166}Os and ^{170}Pt, respectively). Both ^{166}Ir and ^{167}Ir have proton-emitting ground and isomeric states, which also decay by alpha emission. The proton-decay rates have been reproduced by calculations using the WKB barrier penetration approximation and a low-seniority shell-model calculation of the spectroscopic factors. The alpha decays of the four nuclei are followed by chains of alpha decays, allowing the determination of single-particle orbital orderings. Mass information has also been obtained from the alpha-decay chains because a connection to a known mass can be obtained for one of the nuclei. Ground-state mass excesses are reported for ^{151}Tm, ^{154}Yb, ^{155}Lu, ^{158}Hf, ^{159}Ta, ^{162}W, ^{163}Re, ^{166}Os, ^{167}Ir, and ^{170}Pt. The mass excess for ^{171m}Au is also given. Proton separation energies are also deduced for the odd-Z alpha daughter nuclei of the Ir proton emitters. [S0556-2813(97)03205-6]

PACS number(s): 23.50.+z, 21.10.Dr, 25.70.Gh, 27.70.+q

I. INTRODUCTION

For the $Z>72$ odd-Z nuclei lying beyond the proton drip line ($Q_p>0$), the main competing decay modes are alpha and proton emission. Protons experience a relatively low Coulomb barrier and a relatively high centrifugal barrier due to their lower charge and mass compared to alphas. Consequently, decay energy and half-life measurements can be used to determine the orbital angular momentum of the emitted proton for low-lying states in the parent nucleus having simple configurations. In general, this information cannot be obtained for alpha decays in a straightforward way. However, if both an alpha and a proton branch are identified from the same state, the spin assignment obtained from the proton-decay rate can be used to assign states in daughter nuclei populated by unhindered alpha transitions. Furthermore, extended alpha-decay chains can be linked to nuclei having known masses nearer stability, thereby providing mass measurements at the limit of nuclear stability. The above features of this region are exploited with the discovery of new proton radioactivities from ^{165,166,167}Ir and ^{171}Au reported here. In each case it is the proton-decay branch that provides the key to unlocking the door to extensive nuclear structure information. Also, a simple theoretical model is introduced to reproduce systematic trends in proton decay spectroscopic factors between the $Z=64$ and 82 shell closures.

II. EXPERIMENTAL METHOD

The proton emitters were observed in a detection facility associated with the Fragment Mass Analyzer (FMA) [1] at the ATLAS accelerator at Argonne National Laboratory. The FMA is a recoil mass separator which separates 0° reaction products from the primary beam on a microsecond time scale, and disperses them in M/q (mass/charge) at the focal plane.

A thin position-sensitive parallel grid avalanche counter (PGAC) located at the focal plane provides M/q, time of arrival, and energy-loss signals of the recoiling nuclei. After traversing this detector, the ions travel a further 40 cm and are implanted into a double-sided silicon strip detector (DSSD) of thickness 65 μm, area 16×16 mm^2, and having 48 orthogonal strips on the front and rear, respectively [2]. Each strip is instrumented with a charge-sensitive preamplifier, a fast discriminator, and two shaping amplifiers of time-constant 0.5 μs. One amplifier is used for decay events, and has a full-scale output of 20 MeV, while the other has a full-scale output equivalent to 200 MeV, and is used for implant events. Alpha groups from ^{166,167}Os, ^{162,163}W, ^{158,159}Hf, and ^{151}Ho produced during the experiment were used for energy calibration of the decay amplifiers. The proton energies were all obtained with reference to the strong ^{147}Tm ground-state proton transition of energy 1051(3) keV,

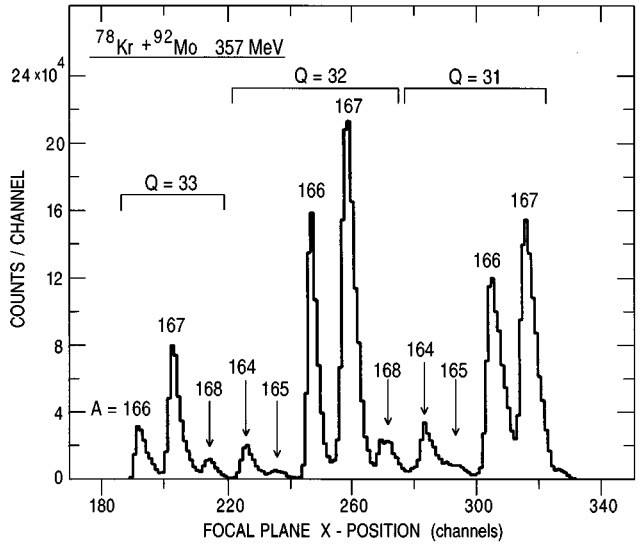

FIG. 1. M/q spectrum for ^{78}Kr+^{92}Mo measured at the FMA focal plane.

produced by bombarding ^{92}Mo with a 261-MeV ^{58}Ni beam in a concurrent experiment.

Events in the DSSD are time-stamped using a 48-bit latching clock operating at 1 MHz, and identified as either an implant (decay) particle, depending on whether they are in coincidence (anticoincidence) with a signal from the PGAC. Reaction recoils are separated from scattered beam events in the DSSD by their energy and time of flight from the PGAC. The 2304 individual x,y quasipixel locations in the DSSD serve as memory cells, allowing the observation of the position and time correlations between the implantation of an individual ion and its subsequent decay products.

The proton emitter ^{171}Au was produced by bombarding a 400 μg/cm^2 isotopically enriched ^{96}Ru target evaporated onto a 700 μg/cm^2 Al backing with 389 MeV ^{78}Kr ions. The proton emitter ^{167}Ir was observed in two reactions. In the first, the above-mentioned ^{96}Ru target was bombarded with a 3 pnA beam of 420 MeV ^{78}Kr for 50 h, producing ^{167}Ir *via* the $\alpha p2n$ evaporation channel. In a subsequent experiment, ^{78}Kr beams of 357 and 384 MeV were used to bombard a 580 μg/cm^2 isotopically enriched ($>$97%) ^{92}Mo target. At the lower energy, ^{167}Ir was produced *via* the $p2n$ evaporation channel, and at the higher energy ^{166}Ir and ^{165}Ir were produced *via* the $p3n$ and $p4n$ channels, respectively.

In this region of the chart of the nuclides, proton emission must compete with alpha decay, having half-lives in the 10–200 ms range, as well as with positron emission and electron-capture decay with half-lives $\geq$0.5 s. Although at first this may seem to be a disadvantage, the capability of observing the subsequent alpha decay of the proton emitter's daughter makes possible the clean identification of even extremely weak proton decay branches.

III. RESULTS AND DISCUSSION

Figure 1 shows a typical M/q spectrum at the focal plane, obtained during the ^{78}Kr+^{92}Mo experiment. The M/q acceptance of the FMA is $\pm$4%, allowing up to three charge states of the same mass to be implanted into the DSSD with essentially uniform illumination.

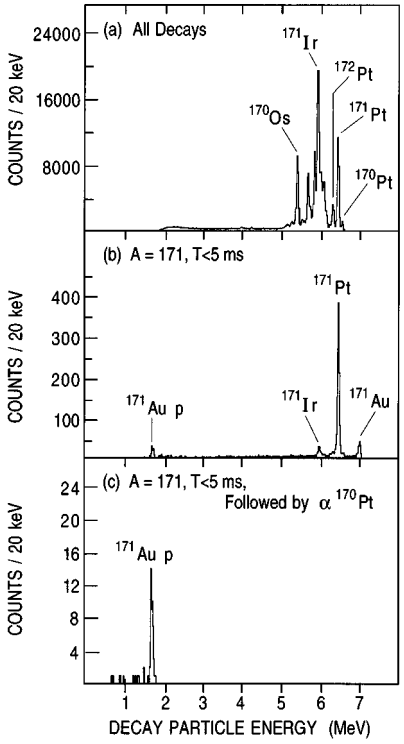

FIG. 2. (a) Energy spectrum of all decay events in the DSSD from 389 MeV ^{78}Kr+^{96}Ru. The peaks above $\sim$5 MeV represent alpha decays, and the broad structure extending down to $\sim$1.8 MeV is due to alphas emitted in the backward direction and only depositing part of their energy before escaping from the DSSD. (b) Same as (a) after requiring that a mass 171 implant was the decay parent and that the decay event occurred in the same pixel within 5 ms of the implantation. (c) Same as (b) subjected to the additional requirements that a subsequent decay event occurred in the same pixel within 20 ms of the first one, with an energy of 6550 keV, the known alpha-decay energy of ^{170}Pt.

A. The decay of ^{171}Au

Figure 2(a) shows the energy spectrum of all decay events in the DSSD from the 389 MeV ^{78}Kr+^{96}Ru run, while Fig. 2(b) shows the same data after requiring that a mass 171 implant was the decay parent and that the decay event occurred in the same pixel within 5 ms of the implantation. The peaks above $\sim$5 MeV represent alpha decays, and the broad structure extending down to $\sim$1 MeV is due to alphas emitted in the backward direction and only depositing part of their energy before escaping from the DSSD. Figure 2(c) shows the data from Fig. 2(b) subjected to the additional requirements that a subsequent decay event occurred in the same pixel within 20 ms of the first one, with an energy of 6550 keV, the known alpha-decay energy of ^{170}Pt. The peak at 1692(6) keV cannot be an alpha particle because of energy considerations, and is therefore identified as a proton from the decay of ^{171}Au. From the time intervals between implantation and decay events, the half-life of the proton group has been determined to be 1.03(15) ms.

Along with the proton group, a new alpha line at 6996(6) keV was observed, associated with mass 171 implants. It was

TABLE I. Proton decay of states in ^{171}Au and ^{165,166,167}Ir.

Nucleus		^{171}Au	^{167}Ir	^{167}Ir	^{166}Ir	^{166}Ir	^{165}Ir
E_p (keV)		1692(6)	1064(6)	1238(7)	1145(8)	1316(8)	1707(7)
Q_p^T (keV)[a]		1718(6)	1086(6)	1261(7)	1168(8)	1340(8)	1733(7)
$t_{1/2}^{\text{expt}}$(ms)		1.02(10)	35.2(20)	30.0(6)	10.5(22)	15.1(9)	0.30(6)
b_p[b]		0.46(4)	0.32(4)	0.004(1)	0.069(29)	0.0176(58)	0.87(4)
$t_{1/2,p}^{\text{expt}}$ (ms)		2.22(29)	110(15)	7500(1900)	152(71)	860(290)	0.35(7)
$t_{1/2,p}^{\text{calc}}$	$s_{1/2}$	38 ns	28.4 ms	162 μs	2.3 ms	23 μs	9.7 ns
	$d_{3/2}$	280 ns	230 ms	1.3 ms	18.2 ms	182 μs	75 ns
	$h_{11/2}$	415 μs	471 s	2.47 s	37 s	341 ms	123 μs

[a]$Q_p^T = E_p$ + recoil energy + screening correction from [4].
[b]Proton branching ratio.

found to be correlated with the known 6410(5) keV alphas from the decay of ^{167}Ir, and has a half-life of 1.02(13) ms. From this correlation measurement, the alpha branching ratio for the state in ^{167}Ir that emits the 6410 keV alpha is $b_\alpha = 0.8(1)$. The cross section for producing ^{171}Au was deduced to be approximately 2 μb.

Since the proton and alpha groups emitted from the decay of ^{171}Au have measured half-lives of 1.03(15) and 1.02(13) ms, it is likely that they come from the same state. Combining these values we obtain a half-life of 1.02(10) ms. It follows from this fast decay that beta decay will be insignificant compared to proton and alpha emission for ^{171}Au. The 1692(6) keV proton group from ^{171}Au has a measured branching ratio of 0.46(4), yielding a proton partial half-life of 2.22(29) ms. The 6996(6) keV alpha group has a branching ratio of 0.54(4).

The available proton orbitals in this region of N and Z are $h_{11/2}$, $d_{3/2}$, and $s_{1/2}$, implying that the protons will be emitted with angular momenta $l=5$, 2, or 0. Table I shows the resulting measured partial proton half-life for ^{171}Au and the values calculated for $s_{1/2}$, $d_{3/2}$, and $h_{11/2}$ proton emission using the WKB barrier transmission approximation, with the real part of the optical model potential obtained from Becchetti and Greenlees [3]. Using other potentials can produce results differing typically by a factor of 2.

In this region of N and Z, proton emission rates are not expected to be enhanced over those calculated using the WKB approximation, so one would expect proton partial half-lives somewhat longer than the calculated ones, but not shorter. A comparison of the measured and calculated proton half-lives in Table I indicates that the 1692(6) keV proton group can only be explained as the $l=5$ decay of the $\pi h_{11/2}$ state of ^{171}Au to the $J=0$ ground state of ^{170}Pt. Interpreting it as an $l=2$ or $l=0$ decay would imply unreasonably large hindrances of 10^3–10^5. The measured partial proton half-life is longer than the calculated value by about a factor of 5. This will be discussed further in Sec. IV below.

Based on results from the decay of ^{167}Ir (see below), we also expect ^{171}Au to have a low-lying $s_{1/2}$ state, unstable to both proton and alpha emission. Since a second proton group was not observed, its half-life must be less than 30 μs, the lower limit of detectability of our equipment. If its half-life were less than 1 μs, the nucleus would decay before reaching the FMA focal plane. Nuclei with half-lives between these values should leave evidence in the DSSD. Those ^{171}Au nuclei in the $s_{1/2}$ state which reach the focal plane and are implanted into the DSSD as $A=171$ recoils would proton decay unobserved. However, the daughter nucleus ^{170}Pt will subsequently decay by alpha emission, and such events will have the ^{170}Pt alpha energy but will be identified as mass 171 implants. We have observed an excess of such events over what would be expected due to random decays, implying a lower limit on the decay half-life for the ^{171}Au($1/2^+$) state of about 1 μs. Using the WKB barrier transmission approximation, this translates to an upper limit on the proton energy of 1.59 MeV. This energy is well below the 1.69 MeV observed for the decay of the $11/2^-$ state, so we identify the $11/2^-$ state as a metastable state in ^{171}Au, with an excitation energy of at least 0.10 MeV. In the same way, an upper limit on the decay half-life of about 30 μs for the ^{171}Au($1/2^+$) state corresponds to a lower limit on the proton energy of 1.43 MeV, and an upper limit on the excitation energy for the $h_{11/2}$ state of 0.26 MeV.

Figure 3 shows the decay scheme deduced for ^{171}Au. The alpha-reduced width for the 6996(6) keV transition, calculated using the method of Rasmussen [5] is 68(8) keV. This value is consistent with an unhindered $\Delta l=0$ transition, and signifies that the decay takes place between $11/2^-$ states in ^{171}Au and ^{167}Ir.

B. The decay of ^{167}Ir

Figure 4(a) shows the decay energy spectrum from the 357 MeV ^{78}Kr+^{92}Mo run. Figure 4(b) shows the same data after requiring that a mass 167 implant was the decay parent and that the decay event occurred in the same pixel within 100 ms of the implantation. Figure 4(c) shows the data from Fig. 4(b) subjected to the additional requirements that a subsequent decay event occurred in the same pixel within 100

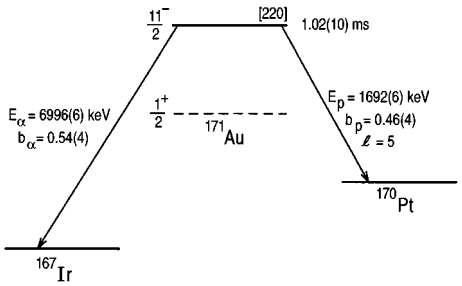

FIG. 3. Decay scheme of ^{171}Au. The estimated excitation energy of the $11/2^-$ state in keV is given in square brackets.

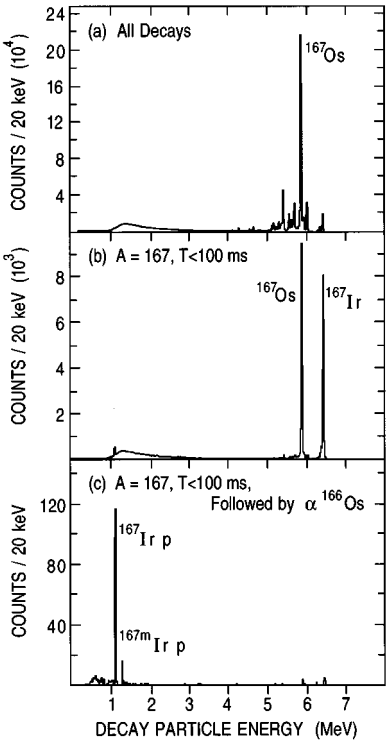

FIG. 4. (a) Decay energy spectrum from 357 MeV ^{78}Kr+^{92}Mo. (b) Same as (a) after requiring that a mass 167 implant was the decay parent and that the decay event occurred in the same pixel within 100 ms of the implantation. (c) Same as (b) subjected to the additional requirements that a subsequent decay event occurred in the same pixel within 100 ms, with an energy of 6000 keV, the known alpha-decay energy of ^{166}Os.

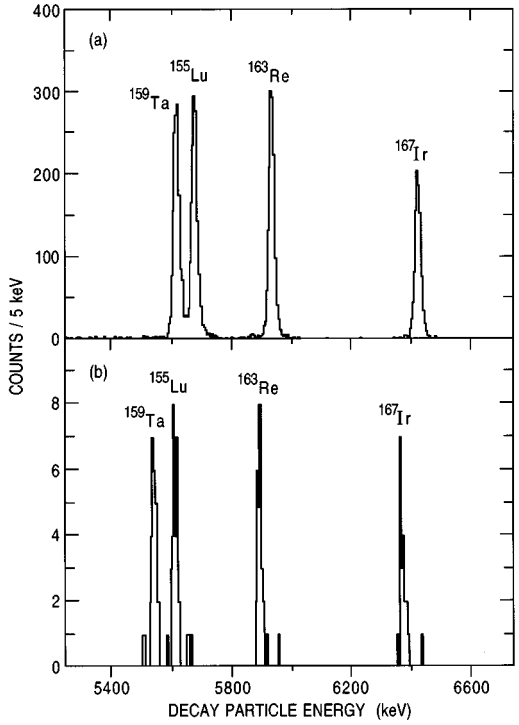

FIG. 5. (a) Energy spectrum of the quadruple-correlated alpha decays terminating with the known 5661 keV transition from ^{155}Lu. This spectrum is the sum of four individual triple-correlated spectra. (b) Same as (a) for the alpha decays terminating with the known 5586 keV ^{155}Lu transition. In both cases the parent nuclei have been assigned by the time ordering of the decays.

ms, with an energy of 6000 keV, the known alpha-decay energy of ^{166}Os. The two peaks at 1064(6) and 1238(7) keV are identified as being from the proton decay of two states in ^{167}Ir. From the time intervals between implantation and decay, the half-lives of the two ^{167}Ir proton groups were obtained. The stronger group at 1064 keV has a half-life of 34.3(22) ms, while the weaker group at 1238 keV has a half-life of 34(9) ms.

In addition to the protons, two alpha lines associated with ^{167}Ir were observed, one strong group with an energy of 6410(5) keV and a previously unobserved weak group at 6351(5) keV. They were each identified by four generations of correlations through ^{163}Re and ^{159}Ta leading to two known alpha groups from the decay of ^{155}Lu. Their measured half-lives are 30.0(6) and 39.7(49) ms. Figure 5(a) shows an energy spectrum of all the alpha decays terminating with the known 5661 keV transition from ^{155}Lu, and Fig. 5(b) shows the decays terminating with the known 5586 keV ^{155}Lu transition. The parent nuclei have been assigned by the time ordering of the decays.

Two proton and two alpha groups are emitted from the decay of ^{167}Ir, all with observed half-lives near 30 ms. Before the measured proton half-lives can be compared with calculation, the proton branching ratios for each state must be obtained. Energy considerations require that the protons be emitted from two states in the parent ^{167}Ir, but populate a common daughter state, the ground state of the even-even nucleus ^{166}Os. We therefore assume that the lowest-energy proton group is emitted from the ^{167}Ir ground state. We associate an alpha group with each of the proton-emitting states in ^{167}Ir. As both states are certainly unbound to alpha emission, it is unlikely that the two alpha groups originate from the same state.

The next task is to determine which proton and alpha groups are associated with each ^{167}Ir state. This cannot be done on the basis of half-lives, because the measured proton and alpha half-lives are so similar. Our results on the alpha decay of the $11/2^-$ state in ^{171}Au showed that it populates an $11/2^-$ state in ^{167}Ir, which decays by emitting the 6410(5) keV alpha. Using our measured Q values for the ^{171}Au alpha and proton decays and for the $^{170}\mathrm{Pt}\rightarrow{}^{166}$Os alpha decay ($E_\alpha = 6550(6)$ keV [6]), we can estimate the proton-decay Q value for the $11/2^-$ state in ^{167}Ir. This is illustrated in Fig. 6. The resulting proton Q value is 1246(11) keV, leading to a proton energy of 1239(11) keV, in remarkably good agreement with the observed value for the higher energy ^{167}Ir group of 1238(7) keV. With the b_α of 0.8(1) for the $11/2^-$ state in ^{167}Ir already determined from the ^{171}Au-^{167}Ir correlation, the measured intensity ratio of the proton group yields a proton branch of 0.004(1). The remaining decay intensity is accounted for by a 0.2(1) beta branch.

Since the stronger alpha line at 6410(5) keV is combined with the weak high-energy proton group at 1238(5) keV, the previously unobserved 6351(5) keV alpha line must be paired with the strong proton line at 1064(6) keV. Assuming a 0.2(1) beta branch for this case as well, we obtain $b_\alpha = 0.48(6)$ and $b_p = 0.32(6)$. Combining the data from both

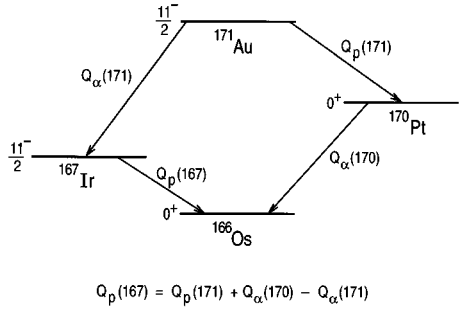

FIG. 6. Q-value loop involving the $11/2^-$ states in ^{171}Au and ^{167}Ir.

proton- and alpha-decay branches gives a half-life of 30.0(6) ms for the metastable state in ^{167}Ir and a half-life of 35.2(20) ms for the ground state. Cross sections for producing the ^{167}Ir states were deduced to be approximately 100 μb for ^{167m}Ir and 10 μb for ^{167g}Ir.

Table I shows the resulting measured partial proton half-lives for ^{167}Ir, and the values calculated for $s_{1/2,}$ $d_{3/2}$, and $h_{11/2}$ proton emission. A comparison of the measured and calculated proton half-lives in Table I indicates that the measured partial proton half-life for the 1064(6) keV proton group is shorter than the values calculated for $d_{3/2}$ and $h_{11/2}$ decay, and can therefore only be explained as the $l=0$ decay of the $\pi s_{1/2}$ ground state of ^{167}Ir. This is the first nucleus for which an $l=0$ ground-state proton decay has been observed. The 1238(7) keV proton group is only consistent with an $l=5$ transition from a low-lying $\pi h_{11/2}$ isomeric state. Both of the measured partial proton half-lives are longer than the calculated value by about a factor of 3. This will be discussed further in Sec. IV below. The assignment of $J=11/2^-$ for the isomeric state is consistent with the expected strong production of ^{167}Ir in high angular momentum states *via* heavy-ion-induced fusion-evaporation reactions. The excitation energy of the isomeric state has been determined to be 175.3(22) keV from the measured proton energy difference, using the peak centroids and the energy dispersion.

Figure 7 shows the decay scheme deduced for ^{167}Ir. Table II gives the energies, half-lives, alpha branching ratios b_α, and alpha reduced widths determined for the alpha transitions from ^{167}Ir and its daughters. The reduced widths were calculated using the method of Rasmussen [5]. The alpha-reduced widths for all of the transitions in Table II are consistent with unhindered $\Delta l=0$ decay, and therefore we assign the 6351 keV line as a $1/2^+\rightarrow 1/2^+$ transition and the

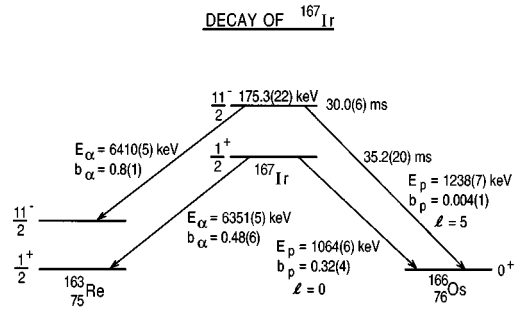

FIG. 7. Decay scheme of ^{167}Ir.

TABLE II. Alpha decays from ^{167}Ir and its daughters.

Parent nuclide	Alpha energy (keV)	Measured half-life (ms)	b_α	Reduced width (keV)
^{167}Ir	6351(5)[a]	35.2(20)	0.48(6)	49(7)
^{167}Ir	6410(5)	30.0(6)	0.8(1)	58(8)
^{163}Re	5870(5)[a]	390(72)	0.32(3)	32(7)
^{163}Re	5920(5)	214(5)	0.66(4)	73(5)
^{159}Ta	5519(5)	830(180)	0.34(5)	59(15)
^{159}Ta	5600(5)	500(11)	0.55(1)	71(2)
^{155}Lu	5586(5)	150(24)	0.76(16)	48(13)
^{155}Lu	5661(5)	63(2)	0.90(2)	66(3)

[a]New alpha activity.

6410 keV line as an $11/2^-\rightarrow 11/2^-$ transition. It is extremely unlikely that an $11/2^-$ state would be able to decay to anything other than a low-lying $11/2^-$ state, but the possibility of a $1/2^+$ state decaying to a $3/2^+$ state cannot be discounted so easily. To check the assignment of the 6351 keV group as an unhindered $1/2^+\rightarrow 1/2^+$ decay, its reduced width was calculated as if it were a hindered $\Delta l=2$ $1/2^+\rightarrow 3/2^+$ decay, resulting in a value of 85(12) keV. Such a large reduced width would have made it faster than any of the unhindered $11/2^-\rightarrow 11/2^-$ alpha decays observed in this experiment, thus ruling out the hindered $\Delta l=2$ $1/2^+\rightarrow 3/2^+$ possibility. The assignment of level orderings to the alpha daughters of ^{167}Ir will be discussed further in Sec. V.

C. The decay of ^{166}Ir

Figure 8(a) shows the energy spectrum of all decay events in the DSSD from the 384 MeV ^{78}Kr+^{92}Mo run, while Fig. 8(b) shows the same data requiring that the decay occurred within 100 ms of a mass 166 implant. Figure 8(c) gives the spectrum correlated with the 6188 keV alpha particles from ^{165}Os. Two proton groups are seen, having energies of 1316(8) and 1145(8) keV, with half-lives of 11.4(58) and 19(9) ms, respectively.

Two alpha groups associated with ^{166}Ir were observed, with energies of 6561(5) and 6562(6) keV. It was only possible to resolve these groups by using the correlation technique. Their measured half-lives are 15.2(9) and 10.2(22) ms. The first group is correlated with the known alphas from the decay of ^{162}Re and ^{158}Ta at 6116 and 6048 keV, respectively. The second, a new weak alpha group, was found to be correlated with two alpha groups, one previously unobserved that we attribute to ^{162}Re, and a known alpha from ^{158}Ta.

In analogy with systematics established closer to stability for the region just above the $Z=64$ and $N=82$ shell closures [7], the odd-odd nucleus ^{166}Ir is expected to have two low-lying states of configuration $[\pi d_{3/2}\nu f_{7/2}]2^-$ and $[\pi h_{11/2}\nu f_{7/2}]9^+$. Two proton and two alpha groups are emitted from ^{166}Ir, with observed half-lives around 10 ms. We assume that they are from two states in ^{166}Ir, each of which emits a proton and an alpha. We also assume that both protons are emitted to the ^{165}Os ground state.

Before the measured proton half-lives can be compared with calculation, the proton branching ratios for each state must be obtained. Using only the half-life information, it is not possible to pair up the protons and alphas. Guided by the

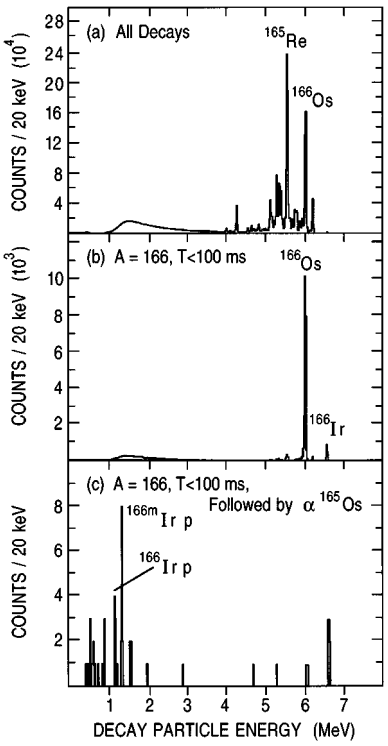

FIG. 8. (a) Energy spectrum of all decay events in the DSSD from 384 MeV ^{78}Kr+^{92}Mo. (b) Same as (a) with the additional requirement that the decay occurred within 100 ms of a mass 166 implant. (c) Same as (b) with the additional requirement that a subsequent decay event occurred in the same pixel within 100 ms with an energy of 6188 keV, the known alpha-decay energy of ^{165}Os.

results from ^{167}Ir, we first postulate that the higher-energy 1316 keV proton and the strong 6561 keV alpha group are emitted from a metastable state with $\pi h_{11/2}$ proton configuration, with the 1145 keV protons and the weak 6562 keV alphas emitted from the ^{166}Ir ground state. These assignments reflect the stronger population of a high-spin state in the heavy-ion fusion reaction and the higher l value needed to slow down the decay rate of a high-energy proton.

Table I shows the resulting measured partial proton half-lives for ^{166}Ir and the values calculated for $s_{1/2}$, $d_{1/2}$, and $h_{11/2}$ proton emission using the WKB barrier transmission approximation. Proton and alpha branches have been calculated assuming a negligible beta branch for either state.

If the high-energy proton group were instead associated with the weaker alpha group, the proton partial half-lives obtained would be 94 ms and 1.5 s, respectively, for the 1316 keV and 1145 keV proton groups. No consistent combination of orbital assignments is possible in this scenario without resorting to unrealistically large hindrances.

Choosing the original combinations cited above, the mean half-life obtained for the metastable state is 15.1(9) ms, and that for the ground state is 10.5(22) ms. The metastable state has a proton branch of 0.0176(58) and an alpha branch of 0.9824(58), while the ground state has a proton branch of 0.069(29) and an alpha branch of 0.931(29). Cross sections for producing the ^{166}Ir states were deduced to be approximately 6 μb for ^{166m}Ir and 0.3 μb for ^{166g}Ir.

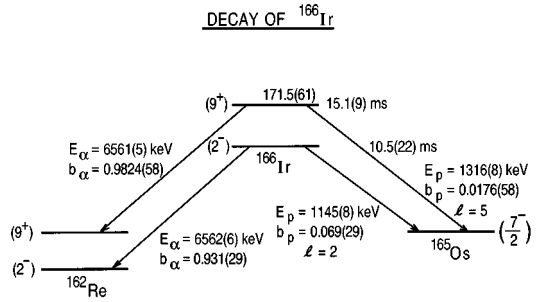

FIG. 9. Decay scheme of ^{166}Ir.

A comparison of the measured and calculated proton half-lives in Table I indicates that the 1145(8) keV proton group can only be explained as the $l=2$ decay of the ground state of ^{166}Ir. This indicates that the protons are emitted from a $d_{3/2}$ orbital. The level of agreement between calculated and measured half-lives is consistent with the results obtained for the other nearby odd-odd nuclides having $d_{3/2}$ proton emitting states, ^{156}Ta and ^{160}Re [8], and will be discussed further in Sec. IV below. The 1316(8) keV group is only consistent with an $l=5$ transition from an $h_{11/2}$ metastable state. Again, the measured proton partial half-life is longer than the calculated value by about a factor of 3. This will be discussed further in Sec. IV below. The assignments for the proton configurations of the two states are consistent with the expected strong production of ^{166}Ir in high angular momentum states *via* heavy-ion-induced fusion-evaporation reactions, and the expectation of low-spin and high-spin states with $d_{3/2}$ and $h_{11/2}$ proton character seems to be borne out. The excitation energy of the isomeric state has been determined to be 171.5(61) keV from these measurements.

Figure 9 shows the deduced decay scheme for ^{166}Ir. Table III gives the energies, half-lives, alpha branching ratios b_α, and alpha-reduced widths determined for the alpha transitions from ^{166}Ir and its daughters. The reduced widths were calculated using the method of Rasmussen [5]. The reduced widths shown in Table III are consistent with all of these alpha transitions being unhindered $\Delta l=0$ transitions.

An alpha-decay scheme for ^{166}Ir is shown in Fig. 10. The excitation energies for the states in ^{162}Re and ^{158}Ta have been calculated from the measured alpha energy differences. The alpha-decaying states have been given preliminary as-

TABLE III. Alpha decays from ^{166}Ir and its daughters.

Parent nuclide	Alpha energy (keV)	Measured half-life (ms)	b_α	Reduced width (keV)
^{166}Ir	6561(5)	15.1(9)	0.9824(58)	43(3)
^{166}Ir	6562(6)[a]	10.5(22)	0.931(29)	58(12)
^{162}Re	6086(5)[a]	107(13)	0.94(6)[b]	48(7)
^{162}Re	6116(5)	84.6(62)	0.94(6)	47(5)
^{158}Ta	5968(5)	72(12)	1.00(8)[c]	31(5)
^{158}Ta	6048(5)	37.7(15)	1.00(8)	29(3)

[a]New alpha activity.

[b]Obscured by other alpha groups; value used is the same as that for the other ^{162}Re line.

[c]Obscured by other alpha groups; value used is the same as that for the other ^{158}Ta line.

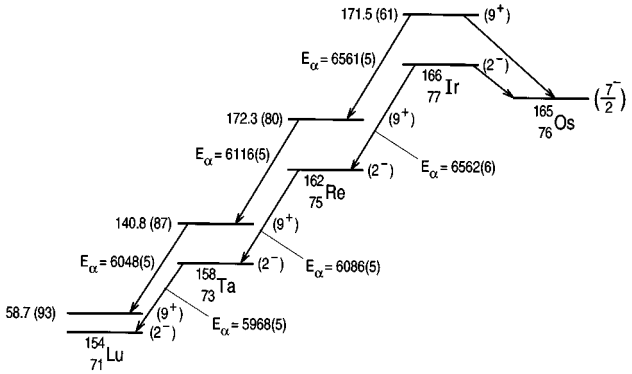

FIG. 10. Decay scheme of correlated alphas from ^{166}Ir.

signments as high-spin (9^+) and low-spin (2^-) isomers.

The three odd-odd nuclei ^{156}Ta, ^{160}Re, and ^{166}Ir are the only proton emitters observed so far in the $N>82$ region that possess a $d_{3/2}$ proton orbital character, even though the $s_{1/2}$ state is either the ground state or a low-lying isomer in the nearby odd-Z odd-A nuclei. This may be explained by applying Nordheim's rules for the coupling of odd neutron and proton particles (or holes). We assume the available low-lying configurations are $[\pi s_{1/2}\nu f_{7/2}]$, $[\pi d_{3/2}\nu f_{7/2}]$, and $[\pi h_{11/2}\nu f_{7/2}]$. In the first case, the weak rule applies, predicting either 3^- or 4^- as the lowest state. The weak rule also applies to the last case, predicting 9^+ or possibly 2^+ as the lowest state. For the $[\pi d_{3/2}\nu f_{7/2}]$ configuration, the strong rule holds, and predicts that a 2^- state will lie far below other states. It is the strong neutron-proton residual interaction that is responsible for the appearance of the $d_{3/2}$ proton orbital in the ground state of ^{166}Ir. The same situation occurs in the odd-odd nucleus ^{154}Tm. The isotone ^{153}Er has a $7/2^-$ ground state, indicating a $\nu f_{7/2}$ character, while ^{153}Tm has an $11/2^-$ ground state, a $1/2^+$ isomer at 43 keV, and a $3/2^+$ state at 135 keV. As suggested by the Nordheim strong rule, the ground-state spin of ^{154}Tm is 2^-. These results indicate that the appearance of $l=2$ proton emission in the $Z>69$ nuclei is not due to a lowering of the $d_{3/2}$ orbital relative to the $s_{1/2}$ orbital.

It is interesting to note that ^{147}Tm is the only odd-A nucleus for which $d_{3/2}$ proton emission has so far been observed [9], and this from an isomeric state. Evidently the single-particle $d_{3/2}$ configuration is not sufficiently bound to produce the ground state. This suggests that a search in the $Z\leqslant 67$ region may reveal further proton emission from this orbital, possibly as hole states.

D. The decay of ^{165}Ir

Figure 11(a) shows the energy spectrum of decay events from the 384 MeV ^{78}Kr+^{92}Mo run, gated by the requirement that the decay occurred within 5 ms of a mass 165 implant. Figure 11(b) gives the spectrum correlated with 6321 keV alpha particles from ^{164}Os. One proton group is seen having an energy of 1707(7) keV and a half-life of 0.29(6) ms. Alpha events with energy 6715(7) keV were also observed, correlated with two generations of known alphas from ^{161}Re and ^{157}Ta. The ^{165}Ir alpha half-life was measured to be 0.39(16) ms.

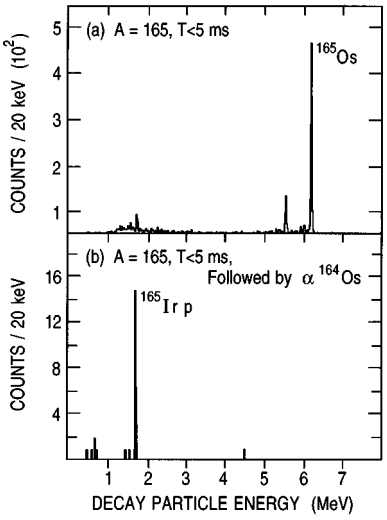

FIG. 11. (a) Energy spectrum of decay events from 384 MeV ^{78}Kr+^{92}Mo, with the requirement that the decay occurred within 5 ms of a mass 165 implant. (b) Same as (a) with the additional requirement that a subsequent decay event occurred in the same pixel within 5 ms, with an energy of 6321 keV, the known alpha-decay energy of ^{164}Os.

Since one proton and one alpha group with similar half-lives were observed in the decay of ^{165}Ir, both particles most likely come from the same state. The mean half-life is 0.30(6) ms. Because of the short half-life, the assumption is made that the beta branch for this state is negligible. A proton branch of 0.87(4) is obtained. The cross section for producing ^{165}Ir was deduced to be approximately 0.2 μb. This is the first case where the reaction product from the $1p4n$ evaporation channel has been observed following a fusion reaction near the proton drip line.

Table I shows the measured partial proton half-life for ^{165}Ir and the values calculated for $s_{1/2}$, $d_{3/2}$, and $h_{11/2}$ proton emission using the WKB barrier transmission approximation. A comparison of the measured and calculated proton half-lives in Table I indicates that the 1707(7) keV proton group can only be explained as an $l=5$ decay of the $\pi h_{11/2}$ state of ^{165}Ir to the $J=0$ ground state of ^{164}Os. Again, the measured partial proton half-life is longer than the calculated value by about a factor of 3. This will be discussed further in Sec. IV below. In analogy with the case of ^{167}Ir, we would also expect a low-lying proton-emitting $s_{1/2}$ state in ^{165}Ir. Using the systematics of the $h_{11/2}-s_{1/2}$ energy differences in ^{153}Lu, ^{157}Ta, and ^{161}Re from [10], we estimate an excitation energy of 0.23(11) MeV for the $h_{11/2}$ state in ^{165}Ir. The estimated decay lifetime for the $s_{1/2}$ ground state of ^{165}Ir is less than 1 μs, too short to be observed.

Figure 12 shows the decay deduced for ^{165}Ir. The 6715(7) keV alpha group from ^{165}Ir has a measured branching ratio of 0.13(4). The alpha-reduced width for this transition, calculated using the method of Rasmussen [5], is 87(32) keV, consistent with an unhindered $\Delta l=0$ transition, and indicating that the decay takes place between $11/2^-$ states in ^{165}Ir and ^{161}Re. This implies that the known 6265(6) keV alpha from ^{161}Re must be from an $11/2^-$ state. Since the known 6213(4) keV alpha from ^{157}Ta was also seen in the correlation, it also must de-excite an $11/2^-$ state.

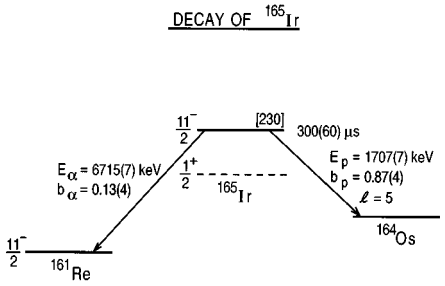

FIG. 12. Decay scheme for ^{165}Ir. The estimated excitation energy of the $11/2^-$ state in keV is given in square brackets.

IV. SPECTROSCOPIC FACTORS AND PROTON HALF-LIVES

The calculation of the proton partial half-life $t_{1/2,p}$ using the WKB barrier transmission approximation does not take into account any nuclear structure effects that might influence the half-life. Although the calculation of the absolute rate for proton decay is simpler than for alpha decay because a preformation factor is not needed, the overlap of parent and daughter states may not be complete. This may occur, for example, when the parent state of an odd-A proton emitter consists of a hole in a particular orbital, while the predominant configuration of the daughter state has this orbital completely filled. The spectroscopic factor is used to described the nuclear structure effects, and is defined as

$$S_j = |\langle \Psi_i(Z+1,A+1)|a^{j\dagger}|\Psi_f(Z,A)\rangle|^2,$$

where $a^{j\dagger}$ is the creation operator for a proton in orbital j.

In an attempt to quantify these ideas, a low-seniority shell-model calculation of the wave functions for the parent and daughter states has been performed, for proton emitters in the $64<Z<82$ region. The model space consisted of 18 particles in the $s_{1/2}$, $d_{3/2}$, and $h_{11/2}$ proton orbitals. The neutron configurations were assumed to be the same for both parent and daughter nuclei, i.e., the neutrons were considered to be spectators. The residual interaction used was a pairing force. In this calculation the single-particle energies for the three orbitals were assumed to be degenerate. Further details of the calculation are found in the Appendix.

Using the resulting wave functions, spectroscopic factors for proton decay of the lowest seniority state in the odd-Z nucleus to the ground state in the daughter were obtained. The results show that the spectroscopic factor depends only on p, the number of pairs of proton holes below $Z=82$ possessed by the daughter nucleus:

$$S(p)=p/9 \quad \text{with} \quad 1\leqslant p\leqslant 9.$$

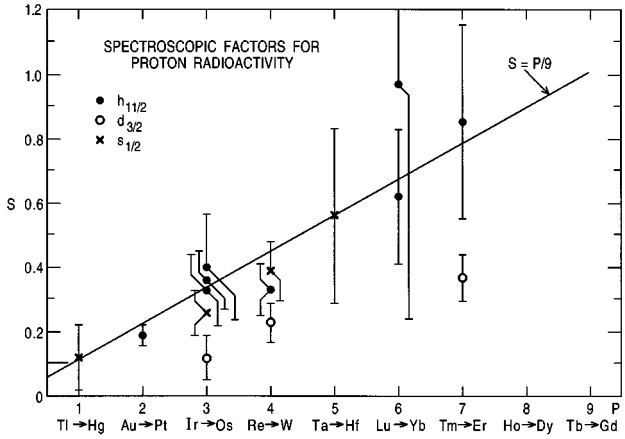

FIG. 13. Spectroscopic factors for new and previously observed proton emitters. In addition to the present work ($^{165(m)}$Ir, ^{167m,g}Ir, ^{171m}Au), data have been taken from [9] (^{147m,g}Tm, ^{151}Lu), [10] (^{157}Ta, ^{161m,g}Re), and [11] (^{177}Tl).

For the cases treated in the present work, $p=2$ for ^{171}Au and $p=3$ for ^{165,166,167}Ir, yielding spectroscopic factors of 0.22 and 0.33, respectively. The experimental spectroscopic factor is defined as the ratio between calculated and measured proton half-life:

$$S^{\text{expt}}=\frac{t_{1/2,p}^{\text{calc}}}{t_{1/2,p}^{\text{expt}}}.$$

Table IV shows the comparison between experimental and calculated spectroscopic factors. The agreement is remarkable, considering the approximations used.

The level of agreement obtained with the simple low-seniority calculation for these nuclei suggests that the model be applied to all the known proton emitters for $65\leqslant Z\leqslant 81$. The results are shown in Fig. 13, indicating that, as predicted, the spectroscopic factors do indeed increase towards 1 as Z approaches 64. The large error bars on the experimental spectroscopic factors for the lighter proton emitters reflects large uncertainties in the beta branches for these nuclei. It is interesting to note that the points showing the largest disagreement with the model are all due to protons decaying from the $d_{3/2}$ orbital.

V. LEVEL ENERGIES AND SPINS FOR STATES IN THE ALPHA-DECAY DAUGHTERS OF ^{167}Ir

Table II shows the alpha decays from ^{167}Ir and its daughters. The 5661 keV transition in ^{155}Lu has previously been assigned as coming from the decay of the $\pi h_{11/2}$ state [12] and Fig. 5(a) shows that it is correlated with the 6410 keV

TABLE IV. Spectroscopic factors for the proton decaying states in ^{171}Au and ^{167,166,165}Ir.

Nuclide	^{171m}Au	^{167g}Ir	^{167m}Ir	^{166g}Ir	^{166m}Ir	$^{165(m)}$Ir
$t_{1/2,p}^{\text{calc}}$	0.415 ms	28.4 ms	2.47 s	18.2 ms	341 ms	0.123 ms
$t_{1/2,p}^{\text{expt}}$	2.22(29) ms	110(15) ms	7.50(190) s	152(71) ms	860(290) ms	0.35(7) ms
S^{calc}	0.22	0.33	0.33	0.33	0.33	0.33
S^{expt}	0.19(3)	0.26(7)	0.33(11)	0.12(7)	0.40(16)	0.36(9)

alpha transition from ^{167}Ir to which we have also assigned the $\pi h_{11/2}$ configuration. Also seen in this decay chain are transitions at 5920(5) keV from ^{163}Re and 5600(5) keV from ^{159}Ta. The reduced widths of these transitions are consistent with their being unhindered transitions, and we assign all of them as connecting $11/2^-$ states.

The other correlated alpha decay chain shown in Fig. 5(b) begins with the 6351(5) keV transition from the $1/2^+$ ground state of ^{167}Ir and ends with the 5586(5) keV transition from ^{155}Lu. The two intermediate alpha transitions, at 5870(5) and 5519(5) keV, are assigned to the decay of states in ^{163}Re and ^{159}Ta. The 5870(5) keV ^{163}Re transition has not been observed previously, while the 5519(5) keV ^{159}Ta transition has been recently reported by Page *et al.* [13]. The branching ratio for the 5586 keV alpha group from ^{155}Lu is measured here. The reduced widths shown in Table II support the idea that all of these alpha transitions are unhindered $\Delta l=0$ transitions.

The odd-Z nuclei in the ^{167}Ir alpha decay chain will have low-lying $d_{3/2}$ and $s_{1/2}$ states. If the alpha decay of the $1/2^+$ ^{167}Ir ground state were to populate the $d_{3/2}$ state in ^{163}Re *via* a hindered $\Delta l=2$ transition, we would also expect to observe a second, unhindered $\Delta l=0$ $1/2^+\rightarrow 1/2^+$ transition. Only one transition has been observed, which further leads us to conclude that this transition is the predominant unhindered $\Delta l=0$ $1/2^+\rightarrow 1/2^+$ transition. This agrees well with previous observation of pairs of $h_{11/2}\rightarrow h_{11/2}$ and $s_{1/2}\rightarrow s_{1/2}$ alpha transitions in nuclei above ^{146}Gd, see, e.g., [14]. Similarly, we conclude that the ^{163}Re and ^{159}Ta transitions occur between $s_{1/2}$ states, which implies from the energetics that these are the ground states of these nuclei. This is consistent with more recent proton radioactivity results obtained at this facility for the neighboring nuclei ^{161}Re and ^{152}Ta, which have $1/2^+$ ground states and $11/2^-$ isomers [10].

There exists the possibility that if the ground state in ^{155}Lu were $3/2^+$, an intermediate gamma transition could occur in ^{155}Lu following the alpha decay of the $1/2^+$ state of ^{159}Ta to the $1/2^+$ state in ^{155}Lu. This would imply that the favored alpha transition from ^{155}Lu would populate the $3/2^+$ state in ^{151}Tm known to be located 108.5 keV above the $1/2^+$ state [15]. However, the energetics of this scenario would imply an $s_{1/2}$ ground state for ^{151}Tm, which is at odds with ground-state systematics for the neighboring Tm isotopes. Both ^{153}Tm and ^{155}Tm have $11/2^-$ ground states and $1/2^+$ isomers. We are therefore led to the conclusion that the low-spin alpha emitted from ^{155}Lu is an unhindered $\Delta l=0$ $1/2^+\rightarrow 1/2^+$ transition.

The full alpha decay chain following the decay of ^{167}Ir is shown in Fig. 14. The excitation energies given in the figure for the isomeric states in ^{163}Re, ^{159}Ta, ^{155}Lu, and ^{151}Tm have been calculated from the measured alpha energy differences. As is seen in Fig. 14, the level ordering of the $1/2^+$ and $11/2^-$ states reverses between ^{159}Ta and ^{155}Lu, indicating that the ground state of ^{155}Lu has spin $11/2^-$. This is consistent with the observation of only ground-state proton radioactivity from the $h_{11/2}$ orbital in ^{151}Lu [9], since proton emission from an excited $s_{1/2}$ state would be too short-lived to be seen.

As can be seen in Fig. 14, the $11/2^- - 1/2^+$ energy differences for the ^{167}Ir alpha-decay chain vary smoothly from negative to positive in going from ^{151}Tm to ^{167}Ir. From this trend we can estimate an excitation energy for the $11/2^-$ state in ^{171}Au of about 0.22(11) MeV, which falls between the lower and upper limits of 0.10 and 0.26 MeV derived independently in Sec. III A.

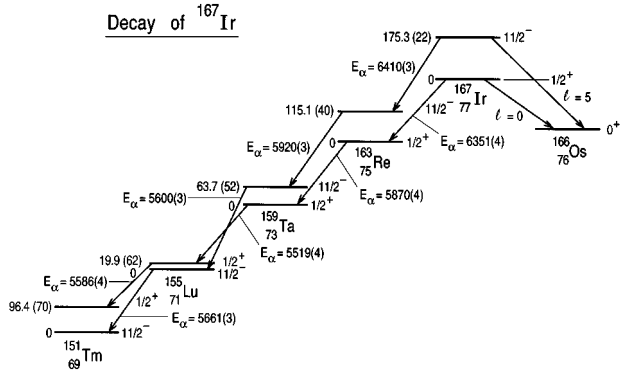

FIG. 14. Decay scheme of correlated alphas from ^{167}Ir.

VI. MASS EXCESSES OBTAINED FROM THE ALPHA AND PROTON DECAYS OF ^{167}Ir

The long alpha-decay chains leading from ^{167}Ir and its proton daughter ^{166}Os eventually terminate on beta-decaying nuclei near the line of stability. If the mass excesses of these beta-unstable nuclei were known, then one could use the alpha- and proton-decay Q values to obtain the mass excesses up to the beginning of the alpha-decay chains. In the case of ^{167}Ir, Fig. 14 shows that the alpha decay terminates with ^{151}Tm. Unfortunately the mass excess of this nucleus is not known.

However, the alpha-decay chain from ^{166}Os terminates on ^{150}Er for which the Q_{EC} to the 2^- state in ^{150}Ho has been measured to be 4108(15) keV [16]. A recent measurement of the mass excess of the ^{150}Ho 2^- state using the ISOLTRAP facility yielded the value $-61950(27)$ keV [17]. The mass excess for ^{150}Er obtained from these two pieces of data is $-57842(31)$ keV, which can be compared with a value of $-57970(100)$ keV obtained from systematics given in the 1995 update to the Atomic Mass Evaluation (AME95) [18].

Table V gives the mass excesses derived for ^{150}Er and ^{154}Yb, ^{158}Hf, ^{162}W, ^{166}Os, and ^{170}Pt, the five known alpha-decay parents of ^{150}Er. A sixth nuclide in the alpha-decay chain, ^{174}Hg, has recently been observed at this facility [19], and will be reported separately. The mass excesses of ^{171m}Au and ^{167}Ir are obtained from their proton-decay energies and the mass excess of ^{166}Os, and are also shown in Table V. The table also shows the systematic predictions from [18] and the differences $\Delta=(M-A)_{\mathrm{expt}}-(M-A)_{\mathrm{AME95}}$.

The ground-state mass excesses of the ^{167}Ir alpha-decay daughters may now be obtained from the ^{167}Ir mass excess, the present alpha-decay Q values, and the decay scheme of Fig. 14. The resulting mass excesses are shown in Table VI. The differences given in Tables V and VI between the experimental mass excesses and those from AME95 show a smooth increase as the isotopes move further from the line of beta stability.

TABLE V. Mass excess values for ^{150}Er and its proton- and alpha-decay parents.

Parent nuclide	Daughter nuclide	Decay Q value (keV)	Daughter $(M\text{-}A)$ (keV)	Parent mass excess (keV)		Δ (keV)
				This work	AME95	
^{150}Er	^{150}Ho(2^-)	4 108(15)[a] (Q_{EC})	−61 950(27)[b]	−57 842(31)	−57 970(100)	128
^{154}Yb	^{150}Er	5 474(2)[a] (Q_α)	−57 842(31)	−49 943(31)	−50 080(100)	137
^{158}Hf	^{154}Yb	5 406(4)[c] (Q_α)	−49 943(31)	−42 112(31)	−42 250(100)	138
^{162}W	^{158}Hf	5 681(5)[c] (Q_α)	−42 112(31)	−34 006(32)	−34 150(100)	144
^{166}Os	^{162}W	6 148(6)[c] (Q_α)	−34 006(32)	−25 433(32)	−25 590(100)	157
^{170}Pt	^{166}Os	6 708(6)[d] (Q_α)	−25 433(32)	−16 300(33)	−16 460(100)	160
^{167}Ir(1/2)	^{166}Os	1 070(6) (Q_p)	−25 433(32)	−17 074(33)	−17 190(100)	116
^{171}Au(1/2)	^{170}Pt	1 702(6) (Q_p)	−16 300(33)	−7 529(115)[e]	−7 660(250)	131

[a]Reference [16].
[b]Reference [17].
[c]Reference [13].
[d]Reference [6], part of the present body of work.
[e]Using an estimated excitation energy of 220(110) keV for the $11/2^-$ state.

VII. PROTON SEPARATION ENERGIES

Given the proton and alpha decay energies of a state in a nucleus (Z,N) and alpha-decay energy of the photon daughter nucleus $(Z-1,N)$, one can calculate the proton-decay Q value Q_p for the analogous state in the alpha daughter nucleus $(Z-2,N-2)$. This procedure has already been described in Sec. III B and illustrated in Fig. 6 for the case of ^{171}Au decay, yielding the Q_p for the $11/2^-$ state of ^{167}Ir. Using the measured proton and alpha energies from the present work and from Ref. [13], we have derived proton separation energies $S_p=-Q_p$ for the odd-Z alpha daughter nuclei of ^{165,166,167}Ir. These are shown in Table VII, along with the measured proton separation energies for the six proton-emitting states obtained in the present experiment. The proton separation energies help to precisely delineate the proton drip line, and allow testing of mass models in the region of the proton drip line.

The proton separation energies derived in Table VII for ^{161}Re(11/2) and ^{157}Ta(11/2) suggest that they are good candidates for proton emission. In fact, proton decay has now been observed at this facility from both of these isotopes, and will be reported separately [10].

Figure 15 shows a comparison between the measured and derived proton separation energies and the mass predictions of Liran-Zeldes [20]. Also shown in the figure are previously obtained proton separation energies for nuclei in this region. The model reproduces the trends in separation energy remarkably well, although it is evident that there is a systematic overestimate of the proton binding by about 200 keV in this region of the drip line. The value shown for ^{171}Au is for $1/2^+$ ground state, lying an estimated 0.22 MeV below its $11/2^-$ state.

VIII. CONCLUSIONS

In the present work, decay properties for new proton-emitting Au ($Z=79$) and Ir ($Z=77$) nuclides have been reported. There is now established a continuous sequence of odd-Z proton emitting isotopes from $Z=69$–79, including the first observation of three proton-emitting isotopes from a single element, Ir. These results have been used to derive shell-orbital orderings, ground-state masses, and proton-decay Q values for isotopes connected together in extended alpha-decay chains. Low-seniority wave functions for the parent and daughter states involved in proton emission for $65\leqslant Z\leqslant 81$ nuclei have been calculated, assuming degenerate single-particle energies for the $h_{11/2}$, $d_{3/2}$, and $s_{1/2}$ proton orbitals, and pairing as a residual interaction. Using these wave functions, spectroscopic factors have been obtained for proton emission. These spectroscopic factors, when combined with proton-decay transition rates calculated using the WKB barrier transmission approximation, agree extremely well with the trend in the experimental decay rates. These results have indicated both the high sensitivity of the correlation technique in identifying the decays of nuclei beyond the proton drip line and the unique detailed nuclear structure information that can be obtained in this region by proton radioactivity studies.

TABLE VI. Mass excess values for the alpha-decay daughters of ^{167}Ir.

Daughter nuclide	Parent nuclide	Decay Q value (keV)	Parent $(M\text{-}A)$ (keV)	Daughter $(M\text{-}A)$ (keV)		Δ (keV)
				This work	AME95	
^{163}Re(1/2)	^{167}Ir(1/2)	6 507(4) (Q_α)	−17 074(33)	−26 006(33)	−26 110(110)	104
^{159}Ta(1/2)	^{163}Re(1/2)	6 018(4) (Q_α)	−26 006(33)	−34 449(33)	−34 550(120)	101
^{155}Lu(11/2)	^{159}Ta(1/2)	5 681(7) ($Q_\alpha+E_x$)	−34 449(33)	−42 555(34)	−42 630(130)	75
^{151}Tm(11/2)	^{155}Lu(11/2)	5 811(4) (Q_α)	−42 555(34)	−50 791(34)	−50 830(140)	39

TABLE VII. Measured and derived proton separation energies.

Nuclide	Proton configuration	Separation energy (keV)	Nuclide	Proton configuration	Separation energy (keV)
^{171m}Au	$h_{11/2}$	−1702(6)[a]	$^{157(m)}$Ta[c]	$h_{11/2}$	−954(14)
^{171g}Au	$s_{1/2}$	−1490(110)[b]	^{155m}Lu	$s_{1/2}$	−120(12)
^{167m}Ir	$h_{11/2}$	−1245(7)[a]	^{155g}Lu	$h_{11/2}$	−99(13)
^{167g}Ir	$s_{1/2}$	−1070(6)[a]	^{154m}Lu	$h_{11/2}$	−268(15)
^{166m}Ir	$h_{11/2}$	−1324(8)[a]	^{154g}Lu	$d_{3/2}$	−208(15)
^{166g}Ir	$d_{3/2}$	−1152(8)[a]	$^{153(g)}$Lu[d]	$h_{11/2}$	−606(15)
^{165m}Ir	$h_{11/2}$	−1717(6)[a,c]	^{151m}Tm	$s_{1/2}$	+141(13)
^{163m}Re	$h_{11/2}$	−826(10)	^{151g}Tm	$h_{11/2}$	+239(14)
^{163g}Re	$s_{1/2}$	−712(9)			
^{162m}Re	$h_{11/2}$	−943(12)			
^{162g}Re	$d_{3/2}$	−770(12)			
$^{161(m)}$Re[c]	$h_{11/2}$	−1315(12)			
^{159m}Ta	$h_{11/2}$	−438(12)			
^{159g}Ta	$s_{1/2}$	−376(11)			
^{158m}Ta	$h_{11/2}$	−594(14)			
^{158g}Ta	$d_{3/2}$	−452(14)			

[a]Measured in the present experiment.
[b]Using estimated $h_{11/2}-s_{1/2}$ energy difference (see text).
[c]Tentatively assigned as a metastable state. Not plotted in Fig. 15.
[d]Tentatively assigned as the ground state.

ACKNOWLEDGMENTS

The authors would like to thank R. L. Chasman and H. Esbensen for valuable discussions, and D. Kurath for performing the shell-model calculation. P.J.W. and T.D. wish to acknowledge travel support from NATO under Grant No. CRG 940303. R.J.I. would like to thank EPSRC for support. Work at Argonne National Laboratory was supported by the U.S. Department of Energy, Nuclear Physics Division, under Contract No. W-31-109-ENG-38. Research at Oak Ridge National Laboratory, which is managed by Lockheed Martin Energy Research Corporation for the U.S. Department of Energy, was supported under contract No. DE-AC05-96OR22464.

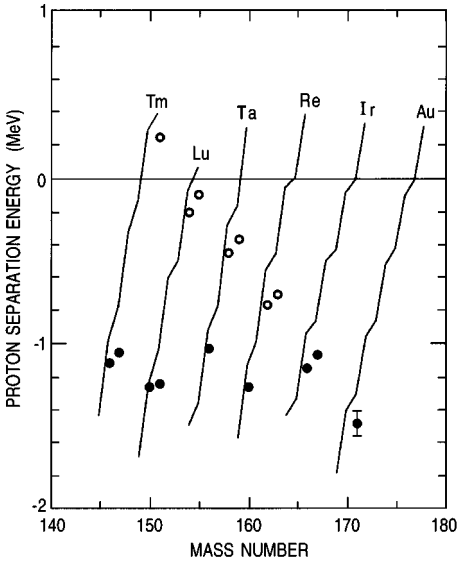

FIG. 15. Proton separation energies for Tm, Lu, Ta, Re, Ir, and Au isotopes. Filled circles denote measured energies, open circles represent derived energies from the present work, and the solid line is the Liran-Zeldes prediction [20]. The value shown for ^{171}Au corresponds to the estimated value for the $1/2^+$ ground state, 1490(110) MeV.

APPENDIX: LOW-SENIORITY SHELL-MODEL CALCULATION FOR PROTON EMITTERS WITH $64<Z<82$

The two-body pairing Hamiltonian has the form

$$H=\sum_j \epsilon_j n_j + G\sum_{j,j'} (-1)^{l+l'}\left[\left(j+\frac{1}{2}\right)\left(j'+\frac{1}{2}\right)\right]^{1/2} \times A^{0\dagger}(j^2)A^0(j'^2),$$

where ϵ_j and n_j are the single-particle energy and the number of particles in orbital j, G is the strength of the pairing interaction, and $A^{0\dagger}(j^2)$ $[A^0(j'^2)]$ is the creation (annihilation) operator for a pair of protons in orbital j coupled to spin 0. The simplifying assumption of degenerate single-particle levels, i.e., $\epsilon_j=\epsilon$, allows the calculation to be performed in the quasispin formalism [21]. Additional details may be found in [22].

Introducing the quasispin raising and lowering operators

$$S^+=\sum_j (-1)^l\left(j+\frac{1}{2}\right)^{1/2} A^{0\dagger}(j^2)$$

and

$$S^- = \sum_{j'} (-1)^{l'} \left(j' + \frac{1}{2} \right)^{1/2} A^{0\dagger}(j'^2),$$

we obtain the quasispin Hamiltonian:

$$H = N\epsilon + \overline{G} S^+ S^-,$$

where

$$N = \sum_j n_j .$$

The quasispin operators obey the same commutation relations as regular angular momentum operators. We have

$$[S^+, S^-] = 2S_0 = N - \sum_j \frac{2j+1}{2} = N - \Omega,$$

where Ω is the total number of pair states. The eigenfunctions of the quasispin operators, with quantum numbers of S and S_z, can be obtained [22] for the lowest seniority state for even and odd Z. In the case of even Z, the lowest seniority $(J=0)$ eigenfunction is

$$\phi^{\,S=\Omega/2}_{S_z=1/2(N-\Omega)}$$

and for odd Z the lowest seniority $(J=j)$ eigenfunction is

$$\phi^{\,S=(\Omega-1)/2}_{S_z=1/2(N-\Omega)}.$$

For the case under study, we have a total of 18 protons in the $d_{3/2}$, $h_{11/2}$, and $s_{1/2}$ orbitals, so $\Omega=9$. Introducing p, the number of proton hole pairs counting down from $Z=82$, the even-Z daughter nuclei have $N=18-2p$, and the odd-Z proton emitters have $N=19-2p$, with $1 \leqslant p \leqslant 9$.

The spectroscopic factor is defined as the overlap between parent and daughter nuclei, and is given by

$$S_j(p) = |\langle \phi^4_{5-p}(J=j) | a^{1/2\dagger}_{1/2}(j) | \phi^{9/2}_{9/2-p}(J=0) \rangle|^2 .$$

This can be reduced to

$$S_j(p) = \left(\frac{9}{2}\,\frac{1}{2}\,\frac{9}{2} - p \;\middle|\; \frac{1}{2}\, 4\, 5-p \right)^2 |\langle \phi^4 \| a^{1/2\dagger} \| \phi^{9/2} \rangle|^2 ,$$

where the p dependence is now contained in the Clebsch-Gordan coefficient. The reduced matrix element can be evaluated for the case of $p=9$, where $S_j(9)=1$, yielding the final result:

$$S_j(p) = \frac{p}{9}.$$

[1] C. N. Davids, B. B. Back, K. Bindra, D. J. Henderson, W. Kutschera, T. Lauritsen, Y. Nagame, P. Sugathan, A. V. Ramayya, and W. B. Walters, Nucl. Instrum. Methods Phys. Res. B **70**, 358 (1992).

[2] P. Sellin *et al.*, Nucl. Instrum. Methods Phys. Res. A **311**, 217 (1992).

[3] F. D. Becchetti and G. W. Greenlees, Phys. Rev. **182**, 1190 (1969).

[4] K.-N. Huang and H. Mark, At. Data Nucl. Data Tables **18**, 243 (1976).

[5] J. O. Rasmussen, Phys. Rev. **113**, 1593 (1959).

[6] C. R. Bingham *et al.*, Phys. Rev. C **54**, R20 (1996).

[7] W. Habenicht, L. Spanier, G. Korschinek, H. Ernst, and E. Nolte, in *Proceedings of the Seventh International Conference on Atomic Masses and Fundamental Constants*, Darmstadt, 1984, edited by O. Klepper [THD Schriftenr. Wiss. Tech. **26**, 244 (1984)].

[8] R. D. Page, P. J. Woods, R. A. Cunningham, T. Davinson, N. J. Davis, S. Hofmann, A. N. James, K. Livingston, P. J. Sellin, and A. C. Shotter, Phys. Rev. Lett. **68**, 1287 (1992).

[9] P. J. Sellin, P. J. Woods, T. Davinson, N. J. Davis, K. Livingston, R. D. Page, A. C. Shotter, S. Hofmann, and A. N. James, Phys. Rev. C **47**, 1933 (1993).

[10] R. J. Irvine *et al.*, Phys. Rev. C **55**, R1621 (1997).

[11] C. N. Davids *et al.* (unpublished).

[12] K. S. Toth and W. Nazarewicz, Phys. Rev. C **48**, R978 (1993).

[13] R. D. Page, P. J. Woods, R. A. Cunningham, T. Davinson, N. J. Davis, A. N. James, K. Livingston, P. J. Sellin, and A. C. Shotter, Phys. Rev. C **53**, 660 (1996).

[14] K. S. Toth, K. S. Vierinen, M. O. Kortelahti, D. C. Sousa, J. M. Nitschke, and P. A. Wilmarth, Phys. Rev. C **44**, 1868 (1991).

[15] P. Kleinheinz, B. Rubio, M. Ogawa, M. Piiparinen, A. Plockhocki, D. Schardt, R. Barden, O. Klepper, R. Kirchner, and E. Roeckl, Z. Phys. A **323**, 705 (1985).

[16] G. Audi and A. H. Wapstra, Nucl. Phys. **A565**, 1 (1993).

[17] D. Beck *et al.* (submitted to Nucl. Phys.).

[18] G. Audi and A. H. Wapstra, Nucl. Phys. **A595**, 409 (1995).

[19] C. N. Davids (private communication).

[20] S. Liran and N. Zeldes, At. Data Nucl. Data Tables **17**, 431 (1976).

[21] A. K. Kerman, R. D. Lawson, and M. H. Macfarlane, Phys. Rev. **124**, 162 (1961).

[22] R. D. Lawson, *Theory of the Nuclear Shell Model* (Clarendon, Oxford, 1980), pp. 76 and 440.